Journal of Structural Geology 138 (2020) 104135

Contents lists available at ScienceDirect

Journal of Structural Geology

journal homepage: http://www.elsevier.com/locate/jsg

# Cartographic pattern of terminations of simple, parallel fault-bend folds, fault-propagation folds and detachment folds

Josep Poblet

*Departamento de Geología, Universidad de Oviedo, C/Jesús Arias de Velasco s/n, 33005, Oviedo, EU, Spain*

ARTICLE INFO

*Keywords:*
Fault-bend fold
Fault-propagation fold
Detachment fold
Geological map
Periclinal termination

ABSTRACT

The maps of terminations of fault-bend folds, fault-propagation folds and detachment folds formed by hinge migration, limb rotation or a combination of both exhibit some differences. In this work, a set of maps has been constructed for simple structures with constant thickness and kink band geometry, and the main differences that allow diagnosing one or another type of structure have been established. Fundamentally, two criteria have been taken into account: geometric differences and differences in the strain distribution on map view. Fault-bend folds and detachment folds formed solely by limb rotation are easily distinguishable, while fault-propagation folds and detachment folds in which hinge migration intervenes are practically identical.

## 1. Introduction

Although many types of fold/thrust interaction have been described in the literature, thrust-related folds are usually classified into three main types: fault-bend folds, fault-propagation folds and detachment folds (e.g., Suppe, 1985; Jamison, 1987; Poblet, 2004; Shaw et al., 2005; Nemcok et al., 2009; McClay, 2011; Brandes and Tanner, 2014). Fault-bend folds and fault-propagation folds are ramp folds because they are related to thrusts in a ramp situation (Fig. 1), whereas detachment folds are related to thrusts in a flat situation (Fig. 2). Fault-bend folds (Rich, 1934) develop as rocks move along non-planar thrust surfaces resulting in rock bending. Fault-propagation folds (Dahlstrom, 1970) develop near the termination of thrusts so that folding and fault propagation are simultaneous. Detachment or décollement folds (Chamberlin, 1910) develop near the tip of thrusts or along thrusts, if fault displacement decreases, and may be limited by lower detachments, upper detachments or both.

Three main kinematic mechanisms have been proposed to account for the amplification of parallel folds: a) folds in which limb dip remains constant and limb length increases through time, so that fold amplification occurs due to hinge migration or kink-band migration (Suppe, 1983); b) folds in which limb length remains constant and limb dip changes through time, and therefore, folds amplify by limb rotation (De Sitter, 1956); and c) folds in which both limb length and limb dip vary through time, so that hinge migration together with limb rotation cause fold amplification (Beutner and DiegeI, 1985). Infinite solutions are possible in the latter case depending on the percentage of contribution of hinge migration versus limb rotation.

The hinge migration mechanism has been successfully applied to fault bend folds (e.g., Suppe, 1983, 1985) and fault-propagation folds (e.g., Suppe and Medwedeff, 1990) (Fig. 1), although mechanisms involving limb rotation have been also proposed for fault-propagation folds (e.g., Mitra, 1990). Detachment folds grow by any of the amplification mechanisms mentioned above, i.e., hinge migration, limb rotation or combination of both mechanisms (e.g., Epard and Groshong, 1995; Homza and Wallace, 1995; Poblet and McClay, 1996) (Fig. 2).

Here I present a set of maps of terminations of different types of simple thrust-related folds with kink-chevron geometries, formed by different amplification mechanisms. These maps have been constructed using serial geological sections across a single structure assuming that cross sections along strike represent different stages of the geometric and kinematic history. The objective of this work is visualizing to what extent the cartographic patterns may be used as a diagnostic element for different types of structures and/or amplification mechanisms. The reason why maps of periclinal terminations of structures have been chosen is because the maps of cylindrical parts of folds, in which the thrust displacement remains constant along strike, are very similar regardless of the type of fold/thrust interaction. On the other hand, this work pretends to be a vindication of the importance of continuing constructing geological maps now that, due to budgetary difficulties and other aspects, geological maps seem to have fallen into obsolescence for some earth science professionals.

Building maps and 3D models of terminations of theoretical folds with kink band and chevron geometries is an old technique developed by

*E-mail address:* jpoblet@geol.uniovi.es.

https://doi.org/10.1016/j.jsg.2020.104135
Received 27 March 2020; Received in revised form 30 June 2020; Accepted 1 July 2020
Available online 6 July 2020

Faill (1973) to analyze the structure of the Appalachians in central Pennsylvania. This strategy has been used in previous works to build 3D block diagrams of theoretical fault-bend folds (Medwedeff, 1989) and fault-propagation folds (Wilkerson et al., 1991), axial surface maps of theoretical fault-bend folds (Shaw et al., 1994), 3D models and maps of theoretical trishear fault-propagation folds (Cristallini and Allmendinger, 2001), contour maps of theoretical fault-bend folds (Bernal and Hardy, 2002), contour maps of theoretical fault-bend, fault-propagation and detachment folds (Salvini and Storti, 2002), and 3D block diagrams and simplified maps of theoretical detachment folds (Wilkerson et al., 2004) amongst others. Although there are several methods to determine the deformation associated with a structure, the criteria used here to define different strain domains are similar to those employed by Salvini and Storti (2001) to construct geological sections across theoretical fault-bend and fault propagation folds.

## 2. Methodology

The assumption that fold geometry variations in space are equivalent to geometric variations in time is an old theory (Elliot, 1976; Means, 1976) that has proved to supply excellent results in some natural examples (e.g., Poblet et al., 1998). One of the great advantages of this theory is that it allows building maps of structures in a simple way. This assumption has been used here for parallel, asymmetric folds, consisting of two planar limbs, a planar crest and very narrow hinges in between them, i.e., with a kink-like geometry (Figs. 1 and 2). The faults related to these folds include a lower detachment, a footwall ramp and an upper detachment in the case of fault-bend folds, i.e., simple-step fault-bend folds, a detachment and a footwall ramp in the case of fault-propagation folds, i.e., simple-step fault-propagation folds, and a detachment in the case of detachment folds. Both the detachments and thrust ramps consist of constant-dip fault surfaces and the transitions from the detachments to the ramps are abrupt. I assumed that the footwalls remain undeformed and are stationary, and therefore, the motion only involves the hangingwalls. Undeformed beds are assumed to be horizontal.

Serial geological sections across different types of fault-related folds formed by different amplification mechanisms have been built in areas with an along-strike gradient of fault displacement decreasing to zero displacement (Figs. 1 and 2). This has allowed constructing geological maps of periclinal terminations of structures. I have assumed that the fault displacement decreases along strike following an arithmetic progression since it is the simplest type of variation. If a geometric progression or another type of function are employed, the main features of the geological maps obtained would be the same although the structure shape would be distorted with respect to the maps constructed using an arithmetic progression. The tectonic transport vector employed is from south to north and the strike of the thrusts is E-W, so that they move as pure dip-slip, reverse faults. In one case the tectonic transport vector is slightly oblique to the thrust strike, and therefore, it behaves like a dip-slip fault with a small strike-slip component; the value of the angle between the tectonic transport vector and the thrust strike has been kept close to 90° to avoid excessive oblique fault displacement. The topography has assumed to be flat in all the sections for simplicity.

The fault geometry and depth, as well as the dip of the limbs, have been kept constant in all the geological sections across fault-bend folds except for two cases. In one of them the lower detachment depth varies and in the other one the thrust dip varies, and in both cases, the change along strike of these two geometric elements follow an arithmetic progression, so that they increase as the thrust displacement increases. The length of the limbs and crest of the fault-bend folds has been modified

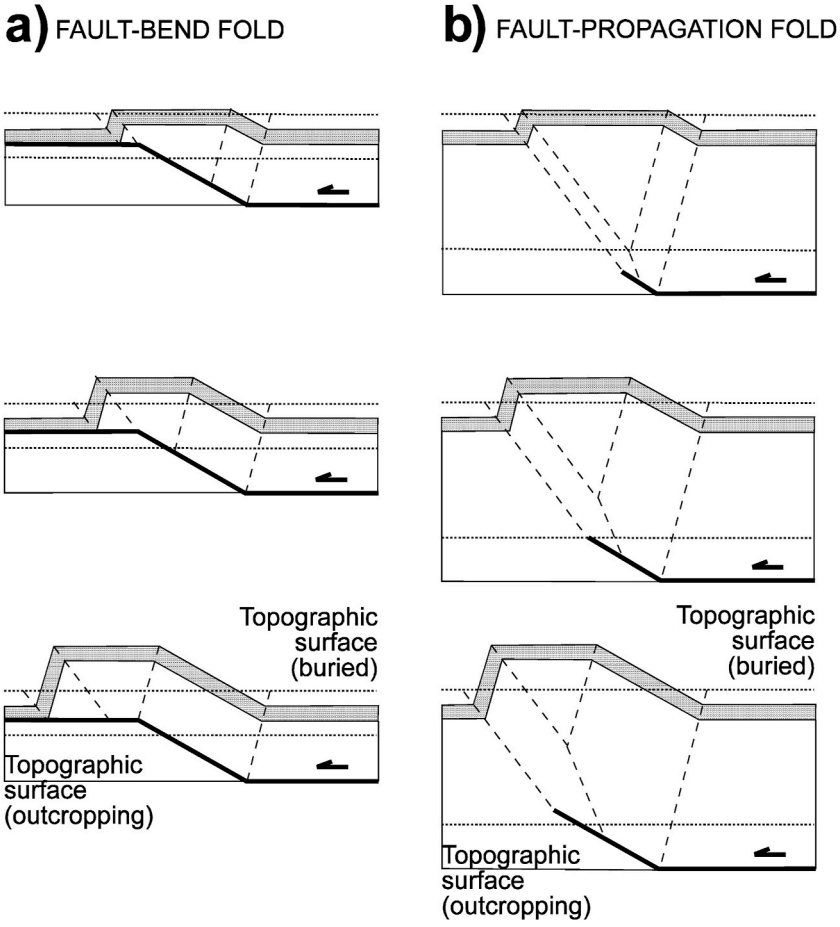


**Fig. 1.** Geological sections across: a) a simple-step fault-bend fold used to build the maps depicted in Fig. 3a and c, and b) a simple-step fault-propagation fold used to build the maps depicted in Fig. 3b and d. The cross sections illustrate different stages of evolution, so that the fault-displacement increases from the upper figures to the lower ones. The upper topographic surface (buried) has been employed to construct the maps depicted in Fig. 3a and b, whereas the lower topographic surface (outcropping thrust) has been employed to construct the maps depicted in Fig. 3c and d.

along strike according to the variations in the amount of fault displacement. The transition from the lower detachment to the footwall ramp and the position of the loose line in the across-strike sections before folding/thrusting have been fixed at the same latitude, except for the case in which the tectonic transport vector is slightly oblique to the thrust strike. The simulated fault-bend folds obey Suppe (1983) equations.

The geometry of the detachment and its depth, as well as the dip of the limbs and footwall ramp, have been kept constant in all the geological sections across fault-propagation folds. The footwall ramp length, as well as the length of the limbs and crest, have been modified according to the thrust-displacement variations along strike. The transition from the detachment to the footwall ramp, as well as the position of the loose line in the across-strike sections before folding/thrusting, has been fixed at the same latitude similarly to fault-bend folds. The simulated fault-propagation folds follow Suppe and Medwedeff (1990) theory.

In the case of detachment folds formed by hinge migration, the dip of the limbs, as well as the forelimb versus backlimb length and the crest length, remained constant in all the geological cross-sections constructed, so that only the length of the limbs varied according to thrust displacement variations. In the case of the limb rotation mechanism, the length of the limbs has been kept constant in all the geological cross-sections, whereas the dip of the limbs varied. In the folds formed by combination of hinge migration and limb rotation mechanisms, only the forelimb versus backlimb length has been kept constant, but the length and dip of the limbs, as well as the crest length, varied along strike. The position of the loose line in the across-strike sections before folding/thrusting has been fixed at the same latitude. The simulated detachment folds correspond to structures developed according to Poblet and McClay (1996) equations.

The maps of subsurface fault-bend folds located in southern California and northeastern Pennsylvania (USA), built by Shaw et al. (1994) using seismic data and techniques different from those used here, are consistent with my maps. This suggests that the methodology employed here to construct the geological maps may be reliable.

The strain distribution is an additional aspect that can help in the diagnosis of different types of fault-related folds. Thus, we have defined different domains within each map by considering the following criteria: a) whether the rocks have or have not been transported along thrust surfaces and/or rotated, b) the number of times rocks rolled though active axial surfaces (Suppe et al., 1992) in the case of folds formed by hinge migration or through limited-activity axial surfaces (Poblet and McClay, 1996) in the case of folds formed by limb rotation, and c) whether the axial surfaces belong to folds with high or low interlimb angles. The strain will be minimum in rocks that have not rolled through any axial surfaces and maximum in rocks that have rolled through two axial surfaces, passing through intermediate values such as when rocks have been transported or rotated, they have rolled through one axial surface whose interlimb angle is high or they have rolled through one axial surface whose interlimb angle is low. Although the strain distribution is controlled by other important factors not considered here, one of the advantages of using the criteria above is its easy applicability.

The strain distribution displayed in sections across fault-bend folds, fault-propagation folds and detachment folds located in outcrops of the Cantabrian Zone (Spain), built by Masini et al. (2010) and Bulnes et al. (2019) using field data and techniques to predict the deformation different from those used here, is consistent with the deformation distribution shown in my maps. This suggests that the methodology employed here to determine the deformation distribution may be reliable.

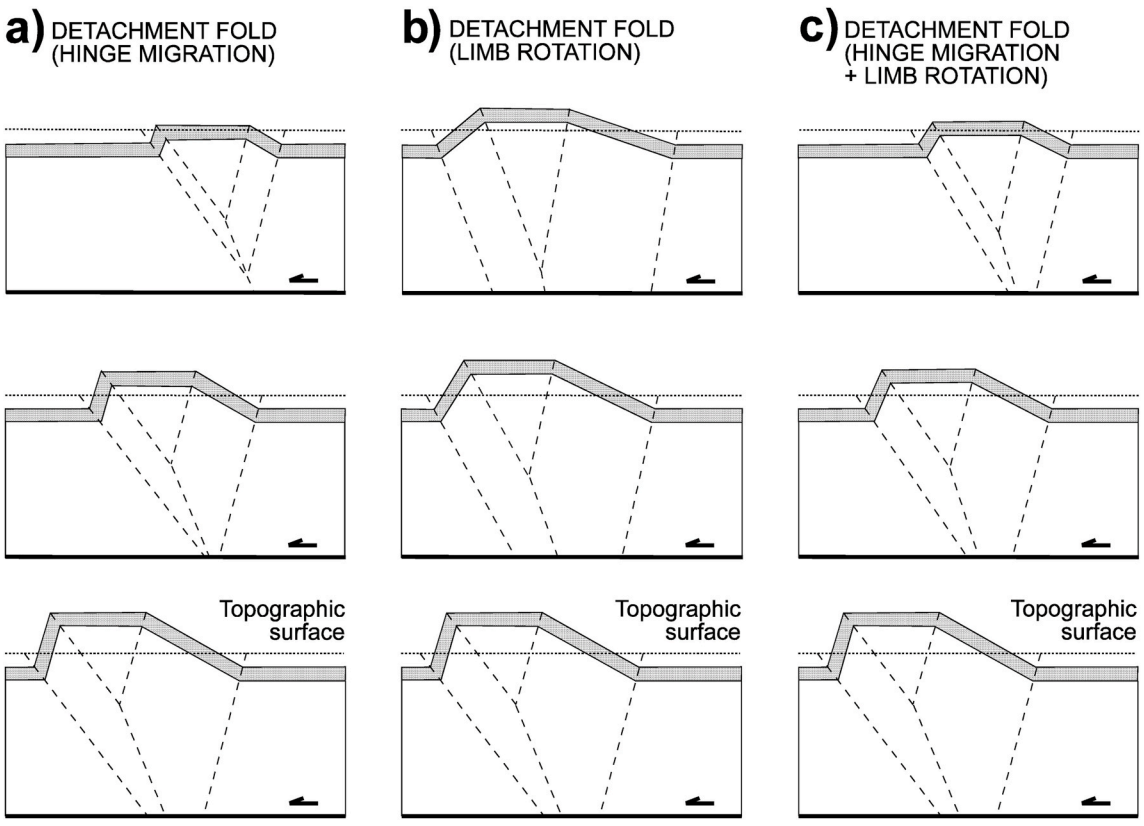


**Fig. 2.** Geological sections across: a) a detachment fold formed by hinge migration used to build the map depicted in Fig. 4a, b) a detachment fold formed by limb rotation used to build the map depicted in Fig. 4b, and c) a detachment fold formed by combination of hinge migration and limb rotation used to build the map depicted in Fig. 4c. The cross sections illustrate different stages of evolution, so that the fault-displacement increases from the upper figures to the lower ones. The topographic surfaces have been employed to construct the maps depicted in Fig. 4.

## 3. Differences between maps of periclinal terminations of thrust-related folds

The differences in terms of geometry of the structures and their strain distribution visualized on maps of periclinal terminations of thrust-related folds, which allow identifying different types and different fold amplification mechanisms, are described below.

### 3.1. Geometry

I will start with maps of periclinal terminations of ramp folds and detachment folds formed on thrusts with constant along-strike geometry and I will compare them. Next, I will examine the influence exerted on the maps by the along-strike variation of each of the three following parameters: the detachment depth, the thrust dip, and the angle between the tectonic transport vector and the thrust strike.

One of the first aspects to highlight is that fold trends in the terminations of structures formed by orthogonal contraction are not always perpendicular to the tectonic transport direction irrespective whether they are ramp folds or detachment folds (Figs. 3–5).

When the thrusts are buried, the trailing and leading anticlinal axial surfaces of the ramp folds get closer as we move towards the central part of the structures (Fig. 3a and b). Regardless of whether the fault-bend fold is in the crestal uplift or crestal widening stage, these two axial surfaces do not join in the case of fault-bend folds leaving a gently dipping or horizontal crest zone in between them, while they end up joining in the case of fault-propagation folds giving rise to a new anticlinal axial surface in the core of the anticline.

The differences between ramp folds when the thrusts crop out are (Fig. 3c and d): a) both the fault-bend fold and the related thrust end in the same transversal because the axial surface that delimits the fold lateral extension and emanates from the thrust tip is perpendicular to the thrust, while the fault-propagation fold extends beyond the end of the thrust because the axial surface that emanates from the thrust tip is oblique to the thrust; b) only the backlimb and crest crop out in the fault-bend fold, while the backlimb, the crest and the forelimb crop out in the fault-propagation fold; and c) the crest of the fault-bend fold is in contact with the thrust, while the crest of the fault-propagation folds is not.

The difference between the maps of different detachment fold types lies in the fold limbs (Fig. 4). When the hinge migration mechanism intervenes in the fold amplification, the cartographic width of the limbs delimited by the axial surfaces, as well as the cartographic width of the folds, decrease towards their termination. On the contrary, when the amplification mechanism is solely limb rotation, the width of the limbs on the map, delimited by the axial surfaces, remains approximately constant along strike and the width of the whole fold decreases towards the central part of the structure.

An important distinction worth noting between ramp and detachment folds is that the traces of the trailing and leading synclinal axial surfaces are not parallel in ramp folds (Fig. 3). This is because the trailing syncline is pinned to the flat-ramp transition, so it reflects the ramp geometry, whereas the forelimb trace is a function of the slip gradient. The trace of the trailing synclinal axial surface tracks that of the leading synclinal axial surface in detachment folds (Fig. 4), because both are a function of the slip gradient.

From the considerations above it follows that it is possible to differentiate three types of structures using the geometrical features depicted on maps of periclinal terminations: fault-bend folds (Fig. 3a and c), fault-propagation folds and detachment folds involving hinge migration (Figs. 3b, d, 4a and 4c), and detachment folds formed by solely limb rotation (Fig. 4b). Fault propagation folds and detachment folds in which hinge migration intervenes are almost indistinguishable

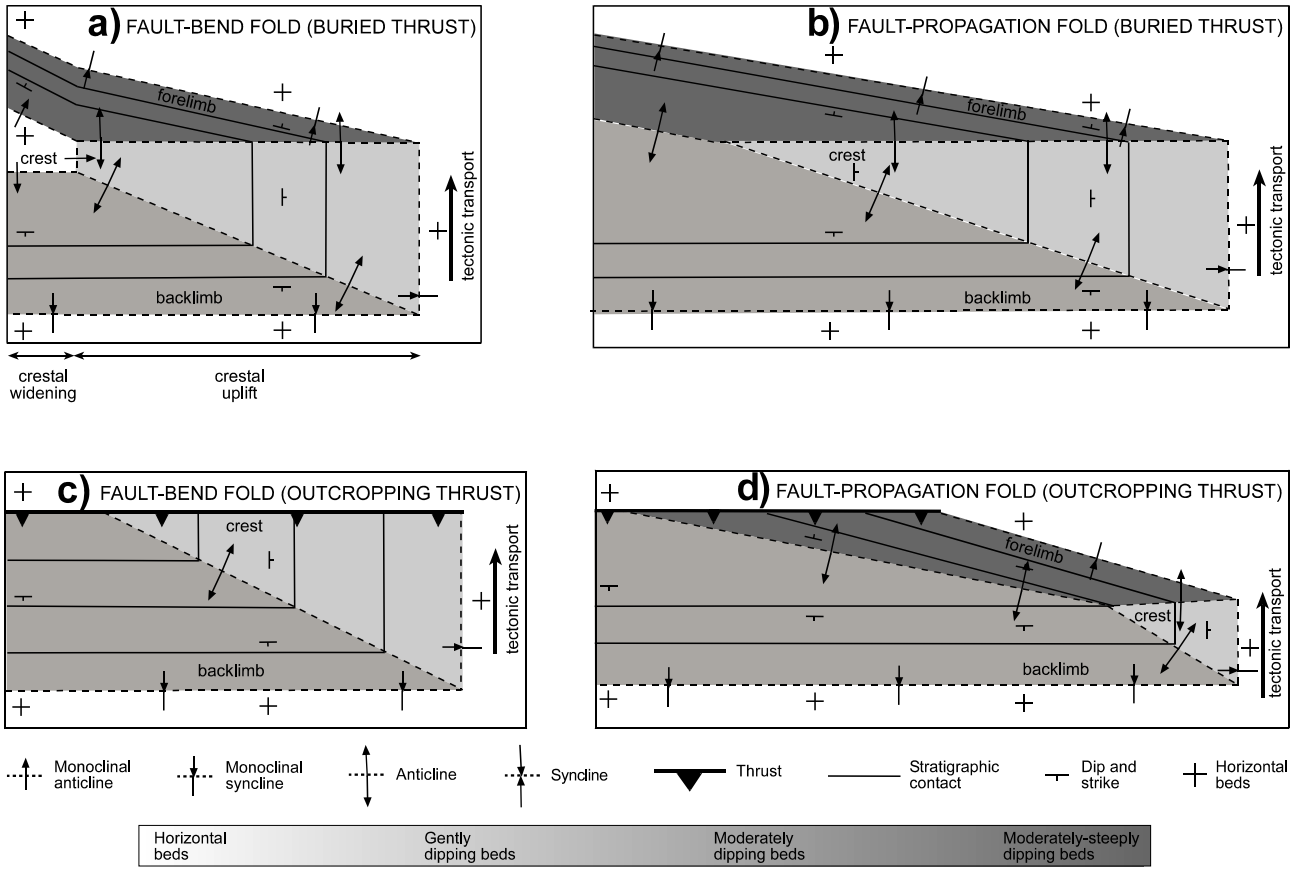


**Fig. 3.** Maps of periclinal terminations of ramp folds formed by orthogonal contraction when the thrusts are buried: a) fault-bend fold and b) fault-propagation fold, and when the thrusts crop out: c) fault-bend fold and d) fault-propagation fold, all of them derived from the cross sections illustrated in Fig. 1.

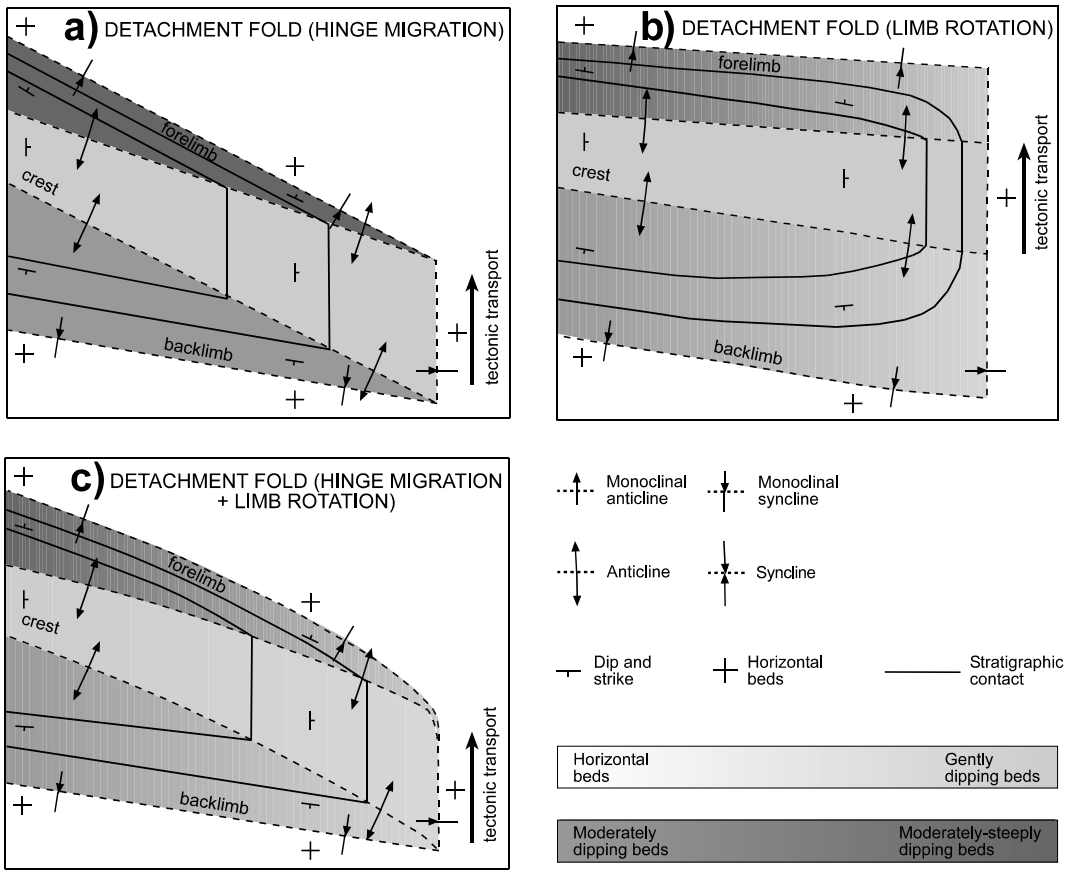


**Fig. 4.** Maps of periclinal terminations of detachment folds formed by orthogonal contraction: a) fold formed by hinge migration, b) fold formed by limb rotation, and c) fold formed by combination of hinge migration and limb rotation, all of them derived from the cross sections illustrated in Fig. 2.

unless the thrusts responsible for the fault-propagation folds crop out.

The maps of the periclinal terminations of fault-bend folds in which the detachment depth varies (Fig. 5a) and those of fault-bend folds formed on thrusts with constant along-strike geometry (Fig. 3a) exhibit two main differences. Thus, the crest of the structure is never horizontal and none of the axial surfaces is parallel to the trailing synclinal axial surface when the detachment depth varies. If the lower detachment depth increases as the thrust displacement increases, then the trailing anticlinal axial surface will progressively separate from the trailing synclinal axial surface so that the backlimb will be wider as the displacement increases (Fig. 5a). In this case, the map is relatively similar to that of fault-propagation folds (Fig. 3b) and of detachment folds involving hinge migration (Fig. 4a–c) because no horizontal crest occurs. Conversely, if the lower detachment depth decreases as the thrust displacement increases, then the backlimb will become narrower for some thrust displacement values.

The main difference between the maps of periclinal terminations of fault-bend folds in which the thrust dip varies along strike (Fig. 5b) and those of fault-bend folds formed on thrusts with constant along-strike geometry (Fig. 3a) is the angle between the leading axial surfaces and the trailing synclinal axial surface. If the thrust dip increases as the thrust displacement increases, the separation between the leading axial surfaces and the trailing synclinal axial surface will increase towards the fold termination (Fig. 5b). If the thrust dip decreases as the thrust displacement increases, the separation between the leading axial surfaces and the trailing synclinal axial surface will decrease towards the fold termination.

The maps of periclinal terminations of ramp folds in which the tectonic transport vector is oblique to the thrust strike (Fig. 5c) exhibit one main difference with respect to those in which the tectonic transport vector is perpendicular to the thrust strike (Fig. 3a). Thus, the trailing synclinal axial surface is oblique to the transverse syncline axial surface that marks the fold lateral end in the former ones and perpendicular in the latter. When the angle measured clockwise from the trailing synclinal axial surface to the transverse synclinal axial surface is acute, the thrust will be a reverse fault with a right-lateral component (Fig. 5c). The maps of these structures are somewhat similar to those of detachment folds involving hinge migration (Fig. 4a–c), although the latter do not have a horizontal crest zone. If the angle measured clockwise from the trailing synclinal axial surface to the transverse synclinal axial surface is obtuse, then the thrust will be a reverse fault with a left-lateral component.

### 3.2. *Strain distribution*

First, I will describe the strain patterns in ramp folds and detachment folds caused by longitudinal axial surfaces and I will compare them. Next, I will discuss the influence exerted on the maps by transverse axial surfaces.

In ramp folds, both fold limbs have rolled once through active axial surfaces; one separates the backlimb from the horizontal rocks transported over the lower detachment and its interlimb angle is high, and another separates the forelimb from the fold crest and its interlimb angle is low (Fig. 6). However, in fault-bend folds in a crestal widening stage, the portion of the fold crest adjacent to the forelimb has not rolled through any active axial surface but the portion of the fold crest adjacent to the backlimb has rolled through two active axial surfaces (Fig. 6a), while the crest of fault-propagation folds has not rolled through any active axial surface (Fig. 6b). The horizontal rocks located beyond the forelimb have been transported over the upper detachment in fault-bend folds (Fig. 6a), while they have remained stationary in fault-propagation folds (Fig. 6b). While both complete fold limbs have rolled once through

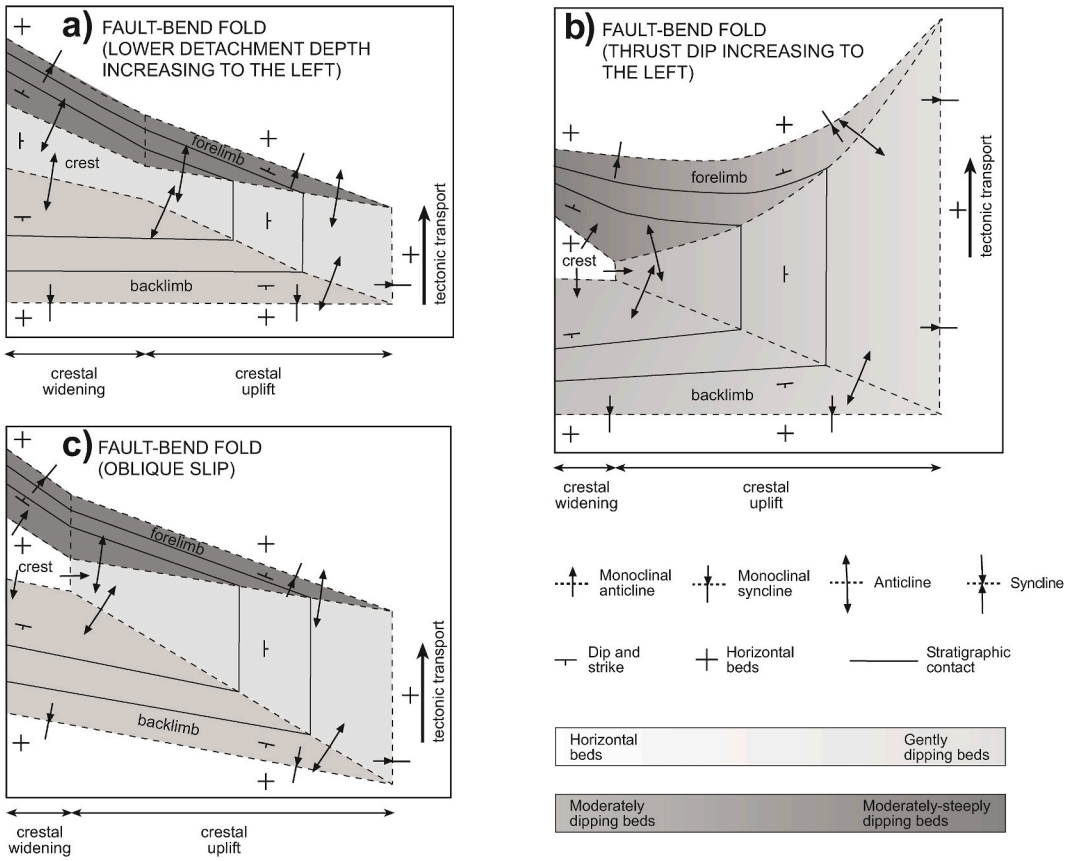


**Fig. 5.** Maps of periclinal terminations of fault-bend folds formed by orthogonal contraction when: a) the lower detachment depth increases from right to left but both the upper detachment depth and the thrust dip remain constant along strike, and b) the thrust dip increases from right to left but the depth to the lower and upper detachment remain constant along strike. c) Map of a periclinal termination of a fault-bend fold whose angle between the thrust strike and the tectonic transport vector is 10°.

active axial surfaces in detachment folds formed by hinge migration (Fig. 7a), only small strips of rocks located in the fold limbs and crest adjacent to the axial surfaces have rolled once through axial surfaces of limited activity in detachment folds formed by limb rotation (Fig. 7b). The horizontal rocks located behind the backlimbs have been transported over the detachment, while those beyond the forelimbs have remained stationary because the detachment folds developed above thrust tips (Fig. 7).

As with geometry, strain distribution maps allow differentiating three types of structures: fault-bend folds (Fig. 6a), fault-propagation folds and detachment folds involving hinge migration (Figs. 6b and 7a), and detachment folds formed by limb rotation (Fig. 7b). Fault-propagation folds and detachment folds in which hinge migration participates are very similar and undistinguishable based on strain distribution maps.

Only active, limited-activity and inactive axial surfaces longitudinal to the structures have been taken into account in the maps presented in Figs. 6 and 7. However, as displacement along the thrusts increases and consequently structures propagate, some areas are also forced to roll through transverse axial surfaces. However, determining which parts of the structures may have rolled through transverse axial surfaces is difficult because these structures may amplify in two different modes described below. a) In the frontal propagation mode, the position of the lateral termination of the structure remains in the same transversal despite increasing the thrust displacement, and therefore, the structure maintains its cartographic length with time (Fig. 8a). Regarding the strain distribution caused by transverse axial surfaces, the most striking aspect of this propagation mode in fault-bend folds is that a portion of the dipping part of the crest rolls through the transverse anticlinal axial surface that separates the dipping part from the horizontal part of the fold crest. Thus, there would be rocks that have rolled through one transverse axial surface in the horizontal part of the fold crest. b) In the frontal propagation combined with along-strike propagation mode, the lateral termination of the structure moves laterally when the displacement along the thrust increases, and therefore, the cartographic length of the structure increases with time (Fig. 8b). Regarding the strain distribution caused by transverse axial surfaces, in addition to that described in the frontal propagation mode, undeformed rocks roll through the transverse synclinal axial surface that bounds the lateral termination of the structure and end up being incorporated into the structure. Thus, apart from rocks that have rolled through one transverse axial surface in the horizontal part of the fold crest, rocks that have rolled through one transverse axial surface would also be found in the dipping part of the fold crest.

## 4. Conclusions

Although the approach presented here is very simple, the geological maps constructed assuming a space-time equivalence yield a general view of the cartographic pattern, in terms of both geometry and deformation distribution, of the periclinal terminations of the most common types of thrust-related folds. Obviously, when the structures are more complex (rounded hinges, footwall involved in the structures, splays emanating from the main thrusts, etc.), the maps are logically more complicated, but even so, the main features should be somewhat similar to those of the maps presented.

These maps may serve as models to be compared with maps of folded and thrusted regions in order to help diagnosing different types of

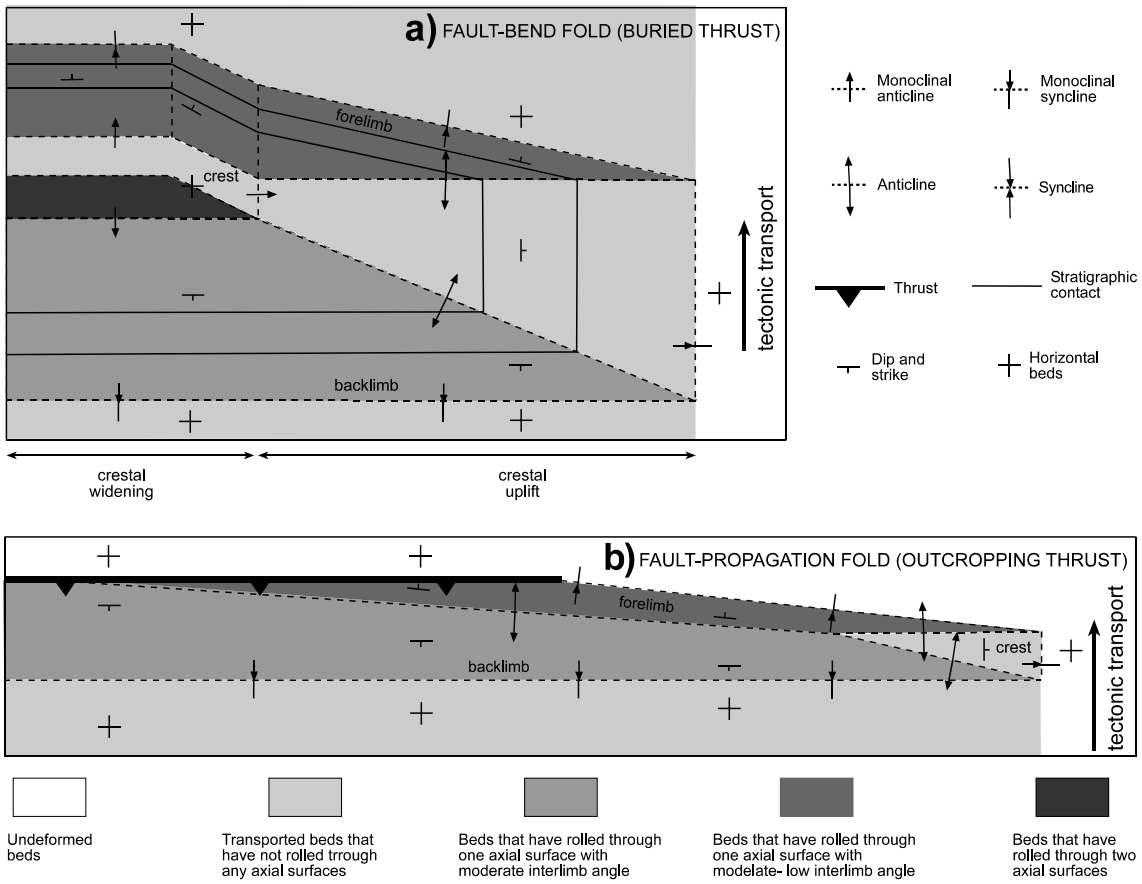


**Fig. 6.** Strain domains superimposed on the maps of periclinal terminations of ramp folds illustrated in Fig. 3: a) fault-bend fold and b) fault-propagation fold with a ramp angle of 29° where the constant thickness and fixed axial-surface theory coincide according to Suppe and Medwedeff (1990). The left side of the fault-bend fold map (Fig. 6a) has been constructed assuming that the fault displacement is constant for better visualization of the strain domain in which rocks have rolled through two axial surfaces. The strain attributed to each of the different domains in the legend increases from left to right, from undeformed rocks to rocks that have rolled through two axial surfaces.

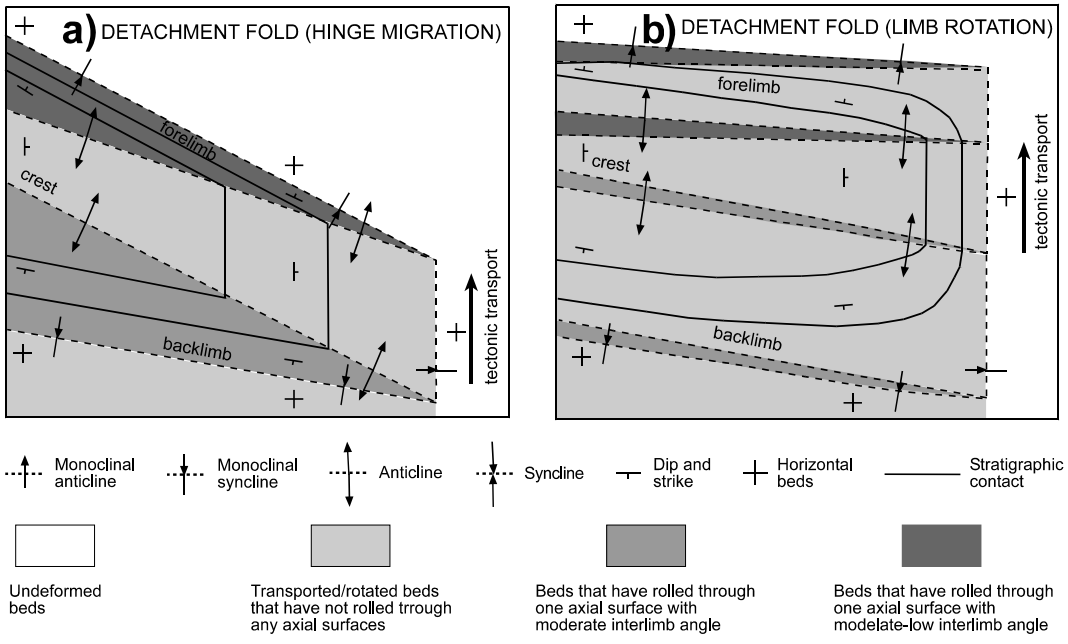


**Fig. 7.** Strain domains superimposed on the maps of periclinal terminations of detachment folds illustrated in Fig. 4: a) fold formed by hinge migration and b) fold formed by limb rotation. The domains in which rocks have rolled through axial surfaces have been slightly enlarged in the map of the detachment fold formed by limb rotation (Fig. 7b) for better visualization. Both detachment folds are developed above thrust tips. The strain attributed to each of the different domains in the legend increases from left to right, from undeformed rocks to rocks that have rolled through an axial surface whose interlimb angle is moderate-low.

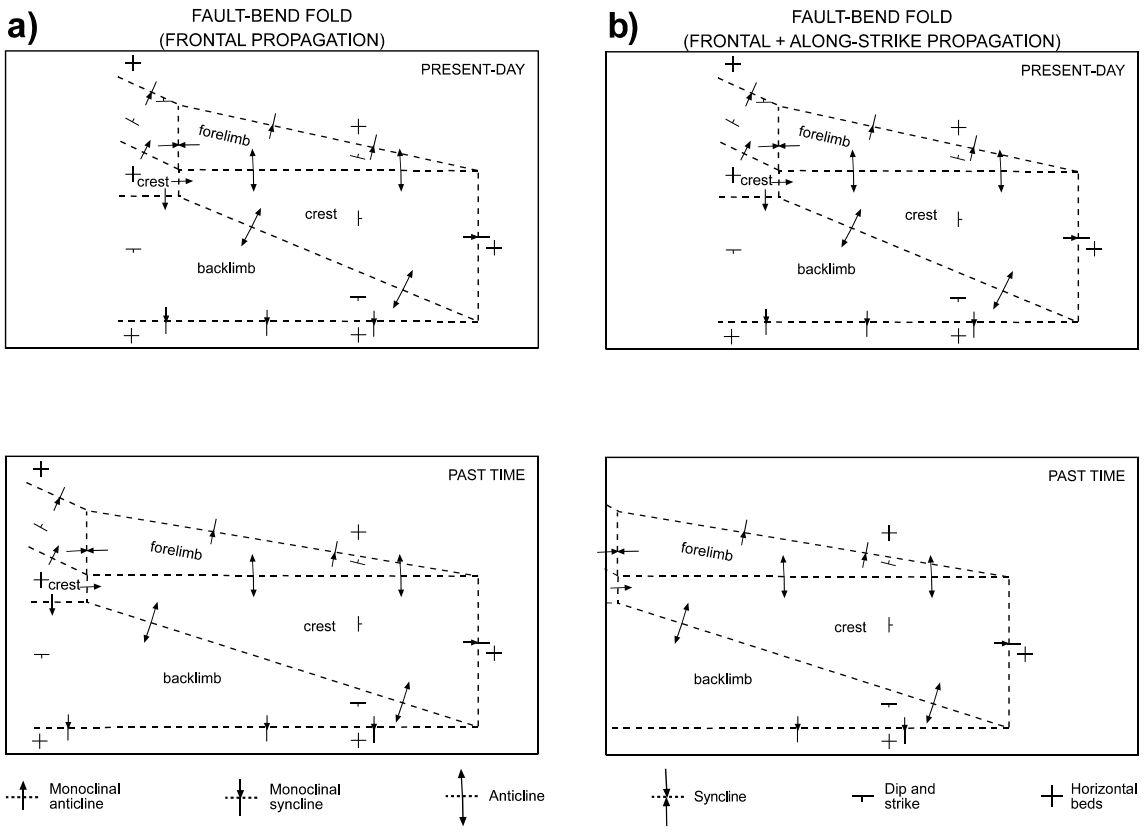


**Fig. 8.** Different modes of propagation of a fault-bend fold formed by orthogonal contraction on map view: a) frontal propagation, and b) frontal plus along-strike propagation, all of them derived from the cross sections illustrated in Fig. 1a. The transverse anticlinal axial surface that separates the horizontal part of the fold crest from the dipping part shifts to the right in both propagation modes with increasing thrust displacement. The transverse synclinal axial surface that marks the lateral termination of the structure shifts to the right only in the frontal combined with along strike propagation mode with increasing thrust displacement.

structures and/or amplification mechanisms, but also as a guide to assist in the construction of geological maps in regions where there is little surface and/or subsurface data (outcrops, well logs, seismics, etc.), the data quality is poor, or the data are unevenly distributed.

## Declaration of competing interest

The authors declare that they have no known competing financial interests or personal relationships that could have appeared to influence the work reported in this paper.

## CRediT authorship contribution statement

**Josep Poblet:** Conceptualization, Methodology, Validation, Formal analysis, Investigation, Writing - original draft, Writing - review & editing, Visualization, Project administration, Funding acquisition.

## Acknowledgements

Comments by Richard Groshong, Chris Connors and the editor, Ian Alsop, have substantially improved the manuscript. I would like to acknowledge financial support by research project CGL2015-66997-R ("Aplicación del análisis del plegamiento a la investigación de recursos geológicos" -AAPLIREGE-) funded by the Spanish Ministry for Economy and Competitiveness and the European Fund for Regional Development (FEDER), as well as research project FC-GRUPIN-IDI/2018/000216 ("Ayudas a organismos públicos de investigación para apoyar la actividad que desarrollen sus grupos de investigación en el Principado de Asturias en el periodo 2018–2020") funded by the Principado de Asturias. I also appreciate the support of many structural geologists and geophysicists from the Geology Department.

## References

Bernal, A., Hardy, S., 2002. Syn-tectonic sedimentation associated with three-dimensional fault-bend fold structures: a numerical approach. J. Struct. Geol. 24 (4), 609–635.
Beutner, E.C., DiegeI, F.A., 1985. Determination of fold kinematics from syntectonic fibers in pressure shadows, Martinsburg slate, New Jersey. Am. J. Sci. 285, 16–50.
Brandes, C., Tanner, D.C., 2014. Fault-related folding: a review of kinematic models and their application. Earth Sci. Rev. 138, 352–370.
Bulnes, M., Poblet, J., Uzkeda, H., Rodríguez-Álvarez, I., 2019. Mechanical stratigraphy influence on fault-related folds development: insights from the cantabrian zone (NW iberian peninsula). J. Struct. Geol. 118, 87–103.
Chamberlin, R.T., 1910. The Appalachian folds of central Pennsylvania. J. Geol. 18, 228–251.
Cristallini, E.O., Allmendinger, R.W., 2001. Pseudo 3-D modeling of trishear fault-propagation folding. J. Struct. Geol. 23 (12), 1883–1899.
Dahlstrom, C.D.A., 1970. Structural geology in the eastern margin of the Canadian Rocky Mountains. Bull. Can. Petrol. Geol. 18 (3), 332–406.
De Sitter, L.V., 1956. Structural Geology. McGraw and Hill, New York.
Elliot, D., 1976. The energy balance and deformation mechanisms of thrust sheets. Royal Soc. London Philosophical Trans. A-283, 289–312.
Epard, J.L., Groshong, R.H., 1995. Kinematic model of detachment folding including limb rotation, fixed hinges and layer-parallel strain. Tectonophysics 247, 85–104.
Faill, R.T., 1973. Kink-band folding, valley and ridge province, Pennsylvania. Bull. Geol. Soc. Am. 84 (4), 1289–1314.
Homza, T.X., Wallace, W.K., 1995. Geometric and kinematic models for detachment folds with fixed and variable detachment depths. J. Struct. Geol. 17, 575–588.
Jamison, W.R., 1987. Geometric analysis of fold development in overthrust terranes. J. Struct. Geol. 9, 207–219.
Masini, M., Bulnes, M., Poblet, J., 2010. Cross-section restoration: a tool to simulate deformation. Application to a fault-propagation fold from the Cantabrian fold and thrust belt, NW Iberian Peninsula. J. Struct. Geol. 32 (2), 172–183.
McClay, K., 2011. Introduction to thrust fault-related folding. In: McClay, K., Shaw, J.H., Suppe, J. (Eds.), Thrust Fault-Related Folding, vol. 94. AAPG Memoir, pp. 1–19.
Means, W.D., 1976. Stress and Strain. Springer Verlag, New York.
Medwedeff, D.A., 1989. Growth Fault-bend folding at southeast lost hills, san joaquin valley, California. AAPG (Am. Assoc. Pet. Geol.) Bull. 73 (1), 54–67.

Mitra, S., 1990. Fault-propagation folds: geometry, kinematics and hydrocarbon traps. AAPG (Am. Assoc. Pet. Geol.) Bull. 74, 921–945.
Nemcok, M., Schamel, S., Gayer, R., 2009. Thrustbelts: Structural Architecture, Thermal Regimes and Petroleum Systems. Cambridge University Press, Cambridge.
Poblet, J., 2004. Geometría y cinemática de pliegues relacionados con cabalgamientos. Trab. Geol. 24, 127–147.
Poblet, J., McClay, K., 1996. Geometry and kinematics of single-layer detachment folds. AAPG (Am. Assoc. Pet. Geol.) Bull. 80, 1085–1109.
Poblet, J., Muñoz, J.A., Travé, A., Serra-Kiel, J., 1998. Quantifying the kinematics of detachment folds using three-dimensional geometry: application to the Mediano anticline (Pyrenees, Spain). Bull. Geol. Soc. Am. 110 (1), 111–125.
Rich, J.L., 1934. Mechanics of low-angle overthrust faulting as illustrated by Cumberland thrust block, Virginia, Kentucky, and Tennessee. AAPG (Am. Assoc. Pet. Geol.) Bull. 18 (12), 1584–1596.
Salvini, F., Storti, F., 2001. The distribution of deformation in parallel fault-related folds with migrating axial surfaces: comparison between fault-propagation and fault-bend folding. J. Struct. Geol. 23 (1), 25–32.
Salvini, F., Storti, F., 2002. Three-dimensional architecture of growth strata associated to fault-bend, fault-propagation, and décollement anticlines in non-erosional environments. Sediment. Geol. 146 (1–2), 57–73.
Shaw, J.H., Hook, S.C., Suppe, J., 1994. Structural trend analysis by axial surface mapping. AAPG (Am. Assoc. Pet. Geol.) Bull. 78 (5), 700–721.
Shaw, J.H., Connors, C.D., Suppe, J., 2005. Part 1: structural interpretation methods. In: Shaw, J.H., Connors, C.D., Suppe, J. (Eds.), Seismic Interpretation of Contractional Fault-Related Folds: an AAPG Seismic Atlas, vol. 53. AAPG Studies in Geology, pp. 1–58.
Suppe, J., 1983. Geometry and kinematics of fault-bend folding. Am. J. Sci. 283, 684–721.
Suppe, J., 1985. Principles of Structural Geology. Prentice Hall, New Jersey.
Suppe, J., Medwedeff, D.A., 1990. Geometry and kinematics of fault-propagation folding. Eclogae Geol. Helv. 83, 409–454.
Suppe, J., Chou, G.T., Hook, S.C., 1992. Rates of folding and faulting determined from growth strata. In: McClay (Ed.), Thrust Tectonics. Springer, Dordrecht, pp. 105–121.
Wilkerson, M.S., Medwedeff, D.A., Marshak, S., 1991. Geometrical modeling of fault-related folds: a pseudo-three-dimensional approach. J. Struct. Geol. 13 (7), 801–812.
Wilkerson, M.S., Wilson, J.M., Poblet, J., Fischer, M.P., 2004. DETACH: an Excel spreadsheet to simulate 2-D cross sections of detachment folds. Comput. Geosci. 30 (9–10), 1069–1077.